Optica Applicata, Vol. LIV, No. 2, 2024
DOI: 10.37190/oa240204

Four-wave mixing model for centrosymmetric constellation shaping in twin-wave-based coherent OFDM system including intersymbol interference

JIANXIN DU*, YU ZHANG, YAJIE XIN

College of Electronic and Optical Engineering & College of Flexible Electronics (Futrue Technology), Nanjing University of Posts & Telecommunication, Nanjing, China

*Corresponding author: dujx@njupt.edu.cn

The four-wave-mixing (FWM) noises are modeled when walk-off and intersymbol interference (ISI) are taken into account for any centrosymmetric constellation shaped signal in orthogonal frequency-division multiplexed (OFDM) with phase-conjugated twin waves (PCTW) scheme. Bit error rate (BER) and the equivalent Q-factor for any constellation shaped signal are also modeled when the FWM and amplified spontaneous emission (ASE) noises are taken into account as additive white Gaussian noise. By using the newly derived semi-analytic models, example calculations are carried out for 16-ary signal in PCTW OFDM system with four cases classified according to some proposed constellation shaping schemes adopted or not. A hybrid constellation shaping scheme consisted of Huffman-coded probabilistic shaping and radius-optimized geometric shaping is proposed. The performance gain in terms of the equivalent Q-factor is calculated to be about 0.563 dB for 16-ary signal in PCTW OFDM system with the proposed hybrid constellation shaping scheme over the square conventional 16QAM signal. The performance degradation for such system due to the effects of ISI on the FWM noise is also evaluated by using the semi-analytic calculation models.

Keywords: CO-OFDM, constellation shaping scheme, four-wave mixing, phase-conjugated twin waves.

1. Introduction

Coherent optical orthogonal frequency-division multiplexed (CO-OFDM) with multi-level subcarrier modulation is an attractive candidate for highly spectral efficient transmission to meet the increasing demand for data transmission capacity, but CO-OFDM applied in optical fiber long haul transmission systems is generally susceptible to fiber nonlinearities owing to high peak to average power ratio (PAPR) [1]. Nonlinear coupling among subcarriers in CO-OFDM systems generates four-wave-mixing (FWM) tones that act as noise, due to randomness of symbol sequences in subcarriers. FWM noise was considered to be the main contribution of performance degradation for such systems [2].

The impact of fiber nonlinearities on the performance of fiber-optic communication system can be reduced by using many techniques such as maximum likelihood sequence estimation (MLSE), digital back propagation (DBP), and model-centric nonlinear equalizer based on the third-order inverse Volterra theory [3-5]. In order to minimize the additional hardware or signal processing, a technique called as phase-conjugated twin waves (PCTW) was proposed [6, 7]. The PCTW scheme denotes that the correlated nonlinear distortions can be coherently canceled by linear superposition in the digital signal processing at the receiver when a signal and its phase-conjugate copy are transmitted on two orthogonal dimensions, respectively. The PCTW technique can be implemented in many domains such as polarization, time slot, subcarrier of OFDM and fiber mode [8-10]. In order to improve the spectral efficiency (SE) which was halved by the conventional PCTW schemes, the dual-PCTW technique with quadrature pulse shaping signals is proposed [11]. Fiber nonlinear tolerance can also be improved by constellation shaping which can be classified as two types. One of them is geometric shaping (GS) which is realized by adjusting the relative position to increase the minimum Euclidean distance between the constellation points [12, 13]. The other is probabilistic shaping (PS) which is realized by changing the constellation probability distribution while maintaining the geometric position [14, 15].

In order to optimize the performance of large-capacity fiber-optic communication system, it is mandatory to evaluate the impact of fiber nonlinear effects on fiber optical system performance [16-18]. It is a huge time-consuming task to evaluate the variance of FWM noise by directly using a well-known spilt step Fourier (SSF) method because many random trials must be run in order to get a good estimate of many random factors such as symbol sequences and initial phases of signals in all subcarriers, so semi-analytical FWM models should be derived by using some statistical methods [19].

Group-velocity walk-off of symbol pulses between channels can greatly influence the impact of FWM noise on system performance, especially for large local dispersion fiber link, so some semi-analytical FWM models including walk-off were proposed for non-return-to-zero on-off keying (NRZ-OOK) format in [20-22]. For other modulation formats such as differential phase shift keying (DPSK), differential quadrature -phase-shift keying (DQPSK), 8-level phase-shift keying (D8PSK) and quadrature amplitude modulation (QAM), the semi-analytical FWM models including walk-off were further developed [23-26]. For CO-OFDM systems with different PCTW schemes, semi-analytic FWM models including walk-off were also developed [27]. For simplicity, the above mentioned semi-analytical FWM models including walk-off have not included the effects of intersymbol interference (ISI) and cannot be used for constellation shaped signal. The ISI comes from the pulse broadening in transmission which is mainly caused by dispersion and fiber nonlinear effects. Including ISI and walk-off, the semi-analytical FWM models are derived in detail in this paper for any constellation shaping signal with self-defined centrosymmetric structure.

Although some Gaussian noise (GN) models including the impacts of fiber nonlinear noises on system performance were proposed for different system scenarios in the past [28], these GN models cannot be directly used for the PCTW OFDM system with any constellation shaping, so semi-analytical models of BER and the equivalent *Q*-factor for such system are proposed in this paper when the total noise including FWM noise is assumed as additive white Gaussian noise.

Four cases of constellation shaping schemes are defined in this paper. The values of the equivalent *Q*-factor for 16-ary PCTW OFDM system with the four cases are evaluated and compared by using the newly derived semi-analytical models. It is shown that Huffman coded probabilistic shaping can be used to greatly improve system performance at the expense of reduced SE regardless of whether geometric shaping is taken into account or not. The improvement of system performance by using the proposed geometric shaping with unchanged SE is relatively limited regardless of whether probabilistic shaping is taken into account or not. It is shown that the optimal values of geometric shaping parameters between the two cases with and without Huffman coded probabilistic shaping are obviously different.

This paper is organized as follows. In Section 2, the centrosymmetric constellation shaped signal is expressed when the effect of ISI due to pulse broadening in transmission is taken into account. In Section 3, the 16-ary signal with Huffman-coded probabilistic shaping and the radius-optimized geometric shaping is expressed. In Section 4, the FWM models for PCTW OFDM system with constellation shaping including ISI are given. In Section 5, the calculation models of BER and the equivalent *Q*-factor for any constellation shaped signal are given. In Section 6, the performance gain is calculated for the proposed constellation shaped 16-ary signal in PCTW OFDM system over the square conventional 16QAM signal without constellation shaping by using the newly semi-analytical calculation models. The performance degradation of 16-ary PCTW OFDM system due to the effects of ISI on the FWM noise is also evaluated for different cases. We summarize our conclusion in Section 7.

2. Expression of centrosymmetric constellation shaped signal including ISI

When the randomness of symbol sequence in the *i*-th subcarrier is taken into account, the electrical field of optical signal for the subcarrier can be expressed as

$$E_i = A_i(t, z)\exp\left\{-j\left[\omega_i t_i - k_i z - \theta_i\right]\right\} + \text{c.c.} \tag{1}$$

$$A(z, t) = L_{\text{CM}} \sum_{j' = -J'}^{J'} \sum_{i' = 0}^{M-1} \varepsilon_{j'}^{(i')} U_{j'}^{(i')} f(j', t, z) \tag{2}$$

where $A(t, z)$ is the slowly varying envelope of the electric field, c.c. denotes complex conjugate, M is the modulation level in this paper, J' is the maximum relative order of symbol which interfere with the given reference symbol due to pulse broadening induced by the effects of dispersion and nonlinearities, i' is the signal constellation order, j' denotes the j'-th symbol in symbol sequence, $U_{j'}^{(i')}$ is the complex amplitude of signal corresponding to the i'-th signal constellation point in the standard constellation, $\varepsilon_{j'}^{(i')}$ is used to describe the occurrence randomness of the i'-th signal constellation point at the j'-th OFDM symbol period, L_{CM} is a ratio between the amplitude of the real signal constellation and that of the standard signal constellation and

$$f(j', t, z) = p\left(t - j'T - \frac{z}{V}\right) H\left(t - \frac{z}{V}, z\right) \tag{3}$$

where $p(t - j'T - z/V)$ is a function describing the pulse shape of the j'-th symbol, $H(t - z/V, z)$ is a window function, T is the OFDM symbol period, V is the group velocity, and

$$H(t) = \begin{cases} 1, & |t| \le \dfrac{T}{2} \\ 0, & \text{otherwise} \end{cases} \tag{4a}$$

$$P_{\mathrm{ave,\ standard}} = \sum_{i'=1}^{M} \left[\langle \varepsilon_{j'}^{(i')} \rangle_{\mathrm{st}} \left| U_{j'}^{(i')} \right|^2 \right] \tag{4b}$$

$$L_{\mathrm{CM}} = \sqrt{\frac{P_{\mathrm{ave}}}{P_{\mathrm{ave,\ standard}}}} \tag{4c}$$

$$Q_{\mathrm{ave,\ standard}} = \sum_{i'=1}^{M} \left[\langle \varepsilon_{j'}^{(i')} \rangle_{\mathrm{st}}^{4} \left| U_{j'}^{(i')} \right|^4 \right] \tag{4d}$$

where P_{ave} is the optical power in each OFDM subcarrier at the launched point of the whole optical fiber link. It can be inferred that $\langle (\varepsilon_{j'}^{(i')})^m \rangle_{\mathrm{st}} = \langle \varepsilon_{j'}^{(i')} \rangle_{\mathrm{st}}$, where m is a positive integer, and the angle bracket $\langle \cdot \rangle_{\mathrm{st}}$ indicates that a quantity is averaged over random variables of symbols. For simplicity of calculation, the signal constellation corresponding to signal complex amplitudes is supposed to be generally centrosymmetric in this paper, which satisfy

$$\langle \sum_{i'=1}^{M} \left[\left(\varepsilon^{(i')} \right) \left(U^{(i')} \right) \right] \rangle_{\mathrm{st}} = 0 \tag{5a}$$

$$\langle \sum_{i'=1}^{M} \left[\left(\varepsilon^{(i')} \right)^2 \left(U^{(i')} \right)^2 \right] \rangle_{\mathrm{st}} = 0 \tag{5b}$$

3. Huffman-coded probabilistic shaping and radius-optimized geometric shaping scheme

Probabilistic shaping can be performed according to the Huffman coding rule. The main Huffman coding process of 16-ary signal is illustrated by Table 1. A geometric shaping

T a b l e 1. Huffman coding for 16-ary signal (A#: input bit sequences, B#: output bit sequences, and C#: the corresponding constellation point).

A#	000	001	100	101	0100	0101	0110	0111
B#	0000	0001	0010	0011	0100	0101	0110	0111
C#	W_0	W_1	W_2	W_3	W_4	W_5	W_6	W_7
A#	11000	11001	11010	11011	11100	11101	11110	11111
B#	1000	1001	1010	1011	1100	1101	1110	1111
C#	W_8	W_9	W_{10}	W_{11}	W_{12}	W_{13}	W_{14}	W_{15}

T a b l e 2. The polar coordinates of the proposed radius-optimized geometric shaped 16-ary signal in the standard constellation, where $A = \arctan(3)$, $B = \arctan(1/3)$, and ε_1, ε_2 and ε_3 are the geometric shaping parameters, ρ and φ are the polar radius and angle, respectively.

	ρ	φ		ρ	φ
W_0	$\sqrt{2} + \varepsilon_1$	$5\pi/4$	W_{12}	$3\sqrt{2} + \varepsilon_3$	$5\pi/4$
W_1	$\sqrt{2} + \varepsilon_1$	$3\pi/4$	W_{13}	$3\sqrt{2} + \varepsilon_3$	$3\pi/4$
W_2	$\sqrt{2} + \varepsilon_1$	$7\pi/4$	W_{14}	$3\sqrt{2} + \varepsilon_3$	$7\pi/4$
W_3	$\sqrt{2} + \varepsilon_1$	$\pi/4$	W_{15}	$3\sqrt{2} + \varepsilon_3$	$\pi/4$
W_7	$\sqrt{10} + \varepsilon_2$	$0 + A$	W_{11}	$\sqrt{10} + \varepsilon_2$	$0 + B$
W_5	$\sqrt{10} + \varepsilon_2$	$\pi/(2 + A)$	W_9	$\sqrt{10} + \varepsilon_2$	$\pi/2 + B$
W_4	$\sqrt{10} + \varepsilon_2$	$\pi + A$	W_8	$\sqrt{10} + \varepsilon_2$	$\pi + B$
W_6	$\sqrt{10} + \varepsilon_2$	$3\pi/(2 + A)$	W_{10}	$\sqrt{10} + \varepsilon_2$	$3\pi/2 + B$

scheme of the 16-ary signal is proposed, which is called as radius-optimized geometric shaping in this paper. The polar coordinates of the geometric shaped 16-ary signal in the standard constellation are shown by Table 2 where ρ and φ are the polar radius and angle, respectively. In Table 2, ε_1, ε_2 and ε_3 are called as the geometric shaping parameters. The radius-optimized geometric shaping scheme of the 16-ary signal can be relatively easily realized by optimizing the values of ε_1, ε_2 and ε_3, while maintaining the polar angles unchanged. As a comparison, the constellation diagram of square conventional 16QAM signals is given (see Fig. 1).

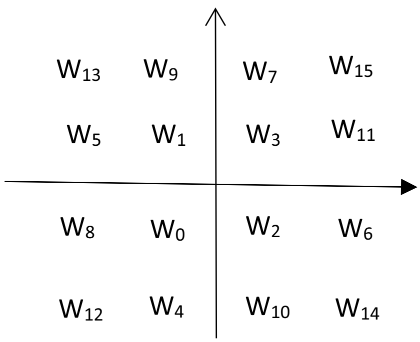

Fig. 1. Constellation diagram of square conventional 16QAM signals.

4. General FWM model including ISI for PCTW OFDM system with constellation shaping

The evolution of the degenerate FWM tone, generated at $\omega_i = \omega_{\mathrm{FWM}} = 2\omega_k - \omega_c$, is given by

$$\frac{\partial A^{\mathrm{D}}_{\mathrm{FWM}(x,\,y)}}{\partial z} + \frac{\alpha}{2} A^{\mathrm{D}}_{\mathrm{FWM}(x,\,y)} \approx j\gamma\Theta_{(x,\,y)} \exp\left[j(\Delta\beta_{\mathrm{D}} z + \Delta\theta_{\mathrm{D}})\right] \tag{6}$$

$$\begin{aligned}\Theta^{\mathrm{D}}_{(x,\,y)} &= A^2_{k(x,\,y)} A^*_{c(x,\,y)} + \frac{2}{3} A_{k(x,\,y)} A_{k(y,\,x)} A^*_{c(y,\,x)} \\ &= A^2_{k(x,\,y)} A^*_{c(x,\,y)} + \frac{2}{3} \left|A_{k(x,\,y)}\right|^2 A^*_{c(y,\,x)}\end{aligned} \tag{7}$$

$$\Delta\theta_D = 2\theta_k - \theta_i - \theta_c \tag{8a}$$

$$\Delta\beta_{\mathrm{D}} = -\beta_2 (2\pi\,\Delta f_{k \to c})^2 \tag{8b}$$

where γ is the nonlinear coefficient, the subscript or superscript of "D" denotes the degenerate FWM case, α is the fiber loss, β_2 is the fiber dispersion, $\Delta f_{k \to c}$ is the subcarrier separation between subcarrier k and c, the subscript x represents the component of a quantity corresponding to the x principal axis direction, while the subscript y represents the component of a quantity corresponding to the y principal axis direction. The equation (6) can be easily solved to obtain the degenerate FWM field at the distance L as

$$A^{\mathrm{D}}_{\mathrm{FWM}(x,\,y)}(t, L) \approx j\gamma \exp\left(-\frac{\alpha}{2}L\right) \int_0^L \Theta_{(x,\,y)} \exp\left[\frac{\alpha}{2}z + j(\Delta\beta_{\mathrm{D}} z + \Delta\theta_{\mathrm{D}})\right] \mathrm{d}z \tag{9}$$

When the coherent superposition of polarization-domain PCTW scheme at the receiver is taken into account, we can obtain

$$A^{\mathrm{D}}_{\mathrm{FWM}} = A^{\mathrm{D}}_{\mathrm{FWM}(x)} + \left(A^{\mathrm{D}}_{\mathrm{FWM}(y)}\right)^* \tag{10}$$

$$\left|A^{\mathrm{D}}_{\mathrm{FWM}}(t, L)\right|^2 = \frac{13}{9} \xi^2_{\mathrm{D}} \left[\sum_{s_k = S_{k(\min)}}^{S_{k(\max)}} A^{\mathrm{D}}_{s_k}(t)\right] \left[\sum_{r_k = S_{k(\min)}}^{S_{k(\max)}} A^{\mathrm{D}}_{r_k}(t)\right]^* \tag{11}$$

where

$$\xi_{\mathrm{D}} = j\gamma L_{c,\,\mathrm{CM}} L^2_{k,\,\mathrm{CM}} \exp\left(-\frac{\alpha}{2}L\right) \tag{12}$$

$$\Lambda_{s_k}^{\mathrm{D}}(t) = \sum_{i'_c = 1}^{M_c} \sum_{j'_c = -J'_c}^{J'_c} \sum_{i''_k = 1}^{M_k} \sum_{j''_k = -J_k}^{J_k} \sum_{i'''_k = 1}^{M_k} \sum_{i'''_k = -J_k}^{J_k} \Big[\varepsilon_{j'_c}^{(i'_c)} \varepsilon_{(s_k - j''_k)}^{(i''_k)} \varepsilon_{(s_k - j'''_k)}^{(i'''_k)} \left(U_{j'_c}^{(i'_c)}\right)^{*} U_{(s_k - j''_k)}^{(i''_k)} U_{(s_k - j'''_k)}^{(i'''_k)} G_{j'_c, s_k, j''_k, j'''_k} \Big] \tag{13}$$

$$G_{j'_c, s_k, j''_k, j'''_k}(t) = g_{j'_c, s_k, j''_k, j'''_k}(t) - g_{j'_c, s_k, j''_k, j'''_k}^{*}(t) \tag{14}$$

$$g_{j'_c, s_k, j''_k, j'''_k}(t) = \int_0^L f(j'_c, t, z) f(j''_k, t'_{s_k}, z) f(j'''_k, t'_{s_k}, z) \exp\left[\left(j\Delta\beta_D + \frac{\alpha}{2}\right) z\right] \mathrm{d}z \tag{15}$$

$$t'_{s_k} = t + s_k T - z / V_k - \tau_k \tag{16}$$

where s_k is a relative number of symbol pulse in k-th subcarrier which is used to describe the walk-off between channels or subcarriers [17], the integers of $S_{k(\min)}$ and $S_{k(\max)}$ are the minimum and maximum values of s_k, the meaning of r_k is similar, $\Lambda_{s_k}^{\mathrm{D}}(t)$ and $\Lambda_{r_k}^{\mathrm{D}}(t)$ are the random parts of FWM tone, the expression of $\Lambda_{r_k}^{\mathrm{D}}(t)$ can be similarly derived, $g_{j'_c, s_k, j''_k, j'''_k}(t)$ is the overlap function corresponding to the degenerate FWM light when the effects of ISI and walk-off on FWM noise are taken into account.

$$P_{(i, c, k)}^{\mathrm{D}} = \frac{13}{9} \gamma (L_{c,\,\mathrm{CM}})^2 (L_{k,\,\mathrm{CM}})^4 \exp(-\alpha L)(T_\Delta)^{-1} \times \int_{-T_\Delta/2}^{T_\Delta/2} \sum_{s_k = S_{k(\min)}}^{S_{k(\max)}} \sum_{r_k = S_{k(\min)}}^{S_{k(\max)}} \sum_{j'_c = -J'_c}^{J'_c} \sum_{j''_k = -J_k}^{J_k} \sum_{j'''_k = -J_k}^{J_k} \sum_{\hat{j}'_c = -J'_c}^{J'_c} \sum_{\hat{j}''_k = -J_k}^{J_k} \sum_{\hat{j}'''_k = -J_k}^{J_k} R_{\mathrm{part}}^{\mathrm{rand}} \, \mathrm{d}t \tag{17}$$

where $R_{\mathrm{part}}^{\mathrm{rand}}$ is the random part of the optical power of FWM noise, and

$$R_{\mathrm{part}}^{\mathrm{rand}} = \sum_{i'_c = 1}^{M_c} \sum_{i''_k = 1}^{M_k} \sum_{i'''_k = 1}^{M_k} \sum_{\hat{i}'_c = 1}^{M_c} \sum_{\hat{i}''_k = 1}^{M_k} \sum_{\hat{i}'''_k = 1}^{M_k} \Bigg\{ \langle \varepsilon_{j'_c}^{(i'_c)} \varepsilon_{\hat{j}'_c}^{(\hat{i}'_c)} \rangle_{\mathrm{st}} \langle \varepsilon_{(s_k - j''_k)}^{(i''_k)} \varepsilon_{(s_k - j'''_k)}^{(i'''_k)} \varepsilon_{(r_k - \hat{j}''_k)}^{(\hat{i}''_k)} \varepsilon_{(r_k - \hat{j}'''_k)}^{(\hat{i}'''_k)} \rangle_{\mathrm{st}} \times \left(U_{j'_c}^{(i'_c)}\right)^{*} U_{(s_k - j''_k)}^{(i''_k)} U_{(s_k - j'''_k)}^{(i'''_k)} G_{j'_c, s_k, j''_k, j'''_k} \left[\left(U_{\hat{j}'_c}^{(\hat{i}'_c)}\right)^{*} U_{(r_k - \hat{j}''_k)}^{(\hat{i}''_k)} U_{(r_k - \hat{j}'''_k)}^{(\hat{i}'''_k)} G_{\hat{j}'_c, r_k, \hat{j}''_k, \hat{j}'''_k}\right]^{*} \Bigg\} \tag{18}$$

For centrosymmetric signal constellation defined in this paper, we can obtain that

$$R_{\text{part}}^{\text{rand}} = \sum_{i_c'=1}^{M_c}\sum_{i_k''=1}^{M_k}\left\{\begin{aligned}&\langle(\varepsilon_{j_c'}^{(i_c')})^2\rangle_{\text{st}}\langle(\varepsilon_{(s_k-j_k'')}^{(i_k'')})^4\rangle_{\text{st}}\left|U_{j_c'}^{(i_c')}\right|^2\left|U_{(s_k-j_k'')}^{(i_k'')}\right|^4\\&\times G_{j_c',s_k,j_k'',j_k'''}\left[G_{\hat{j}_c',r_k,\hat{j}_k'',\hat{j}_k'''}\right]^*\delta_{j_c',\hat{j}_c'}\delta_{s_k,r_k}\delta_{j_k'',j_k'''}\delta_{\hat{j}_k'',\hat{j}_k'''}\end{aligned}\right\}$$

$$+\sum_{i_c'=1}^{M_c}\sum_{i_k''=1}^{M_k}\sum_{i_k'''=1}^{M_k}\left\{\begin{aligned}&\langle(\varepsilon_{j_c'}^{(i_c')})^2\rangle_{\text{st}}\langle(\varepsilon_{(s_k-j_k'')}^{(i_k'')})^2\rangle_{\text{st}}\langle(\varepsilon_{(s_k-j_k''')}^{(i_k''')})^2\rangle_{\text{st}}\\&\times\left|U_{j_c'}^{(i_c')}\right|^2\left|U_{(s_k-j_k'')}^{(i_k'')}\right|^2\left|U_{(s_k-j_k''')}^{(i_k''')}\right|^2 G_{j_c',s_k,j_k'',j_k'''}\left[G_{\hat{j}_c',r_k,\hat{j}_k'',\hat{j}_k'''}\right]^*\\&\times\delta_{j_c',\hat{j}_c'}\delta_{(s_k-j_k''),(r_k-\hat{j}_k'')}\delta_{(s_k-j_k'''),(r_k-\hat{j}_k''')}(1-\delta_{j_k'',j_k'''})\end{aligned}\right\} \tag{19}$$

where δ is the Kronecker delta function, for example,

$$\delta_{(s_k-j_k''),(r_k-\hat{j}_k'')} = \begin{cases}1, & (s_k-j_k''=r_k-\hat{j}_k'')\\0, & (s_k-j_k''\neq r_k-\hat{j}_k'')\end{cases} \tag{20}$$

It can be inferred that

$$\sum_{i_k''=1}^{M_k}\left[\langle(\varepsilon_{(s_k-j_k'')}^{(i_k'')})^2\rangle_{\text{st}}\left|U_{(s_k-j_k'')}^{(i_k'')}\right|^2\right] = \sum_{i_k'''=1}^{M_k}\left[\langle(\varepsilon_{(s_k-j_k''')}^{(i_k''')})^2\rangle_{\text{st}}\left|U_{(s_k-j_k''')}^{(i_k''')}\right|^2\right] \tag{21}$$

Some statistically averaged quantities are defined as

$$P_{c,\text{ ave, standard}} = \sum_{i_c'=1}^{M_c}\left[\langle(\varepsilon_{j_c'}^{(i_c')})^2\rangle_{\text{st}}\left|U_{j_c'}^{(i_c')}\right|^2\right] \tag{22a}$$

$$P_{k,\text{ ave, standard}} = \sum_{i_k''=1}^{M_k}\left[\langle(\varepsilon_{(s_k-j_k'')}^{(i_k'')})^2\rangle_{\text{st}}\left|U_{(s_k-j_k'')}^{(i_k'')}\right|^2\right] \tag{22b}$$

$$Q_{k,\text{ ave, standard}} = \sum_{i_k''=1}^{M_k}\left[\langle(\varepsilon_{(s_k-j_k'')}^{(i_k'')})^4\rangle_{\text{st}}\left|U_{(s_k-j_k'')}^{(i_k'')}\right|^4\right] \tag{22c}$$

we can obtain that

$$R_{\text{part}}^{\text{rand}} = P_{c,\,\text{ave, standard}} Q_{k,\,\text{ave, standard}} \left| G_{j'_c,\, s_k, j''_k, j'''_k} \right|^2 \delta_{j'_c, \hat{j}'_c} \delta_{s_k,\, r_k} \delta_{j''_k, j'''_k} \delta_{\hat{j}''_k, \hat{j}'''_k}$$
$$+ P_{c,\,\text{ave, standard}} P^2_{k,\,\text{ave, standard}} \left| G_{j'_c,\, s_k, j''_k, j'''_k} \right|^2$$
$$\times \delta_{j'_c, \hat{j}'_c} \delta_{(s_k - j''_k),\,(r_k - \hat{j}''_k)} \delta_{(s_k - j'''_k),\,(r_k - \hat{j}'''_k)} (1 - \delta_{j''_k, j'''_k}) \tag{23}$$

and

$$P^{\text{D, part 1}}_{(i,\,c,\,k)} = \frac{13}{9} P_{c,\,\text{ave}} \left(\frac{P_{k,\,\text{ave}}}{P_{k,\,\text{ave, standard}}} \right)^2 Q_{k,\,\text{ave, standard}}\, \gamma \exp(-\alpha L) T_\Delta^{-1}$$
$$\times \int_{-T_\Delta/2}^{T_\Delta/2} \sum_{s_k = S_{k(\min)}}^{S_{k(\max)}} \sum_{j'_c = -J'_c}^{J'_c} \sum_{j''_k = -J_k}^{J_k} \sum_{j'''_k = -J_k}^{J_k} \left[\left| G_{j'_c,\, s_k, j''_k, j'''_k} \right|^2 \delta_{j''_k, j'''_k} \right] \mathrm{d}t \tag{24a}$$

$$P^{\text{D, part 2}}_{(i,\,c,\,k)} = \frac{13}{9} P_{c,\,\text{ave}} P^2_{k,\,\text{ave}}\, \gamma \exp(-\alpha L) T_\Delta^{-1}$$
$$\times \int_{-T_\Delta/2}^{T_\Delta/2} \sum_{s_k = S_{k(\min)}}^{S_{k(\max)}} \sum_{j'_c = -J'_c}^{J'_c} \sum_{j''_k = -J_k}^{J_k} \sum_{j'''_k = -J_k}^{J_k} \left| G_{j'_c,\, s_k, j''_k, j'''_k} \right|^2 (1 - \delta_{j''_k, j'''_k})\, \mathrm{d}t \tag{24b}$$

$$P^{\text{D}}_{(i,\,c,\,k)} = P^{\text{D, part 1}}_{(i,\,c,\,k)} + P^{\text{D, part 2}}_{(i,\,c,\,k)} \tag{24c}$$

The expression of the optical power of non-degenerate FWM noise can be similarly derived.

5. Calculation model of BER and the equivalent *Q*-factor for any constellation shaping

When the total noise is assumed as additive white Gaussian noise, the Gaussian probability density functions of the total noise can be derived as follows:

$$d^{(i,\,k)} = \sqrt{\left(n_{\text{I}} + S_{\text{I}}^{(i)} + S_{\text{I}}^{(k)}\right)^2 + \left(n_{\text{Q}} + S_{\text{Q}}^{(i)} + S_{\text{Q}}^{(k)}\right)^2} \tag{25}$$

$$P_{\text{ro}}^{(i,\,j)} = \iint_{-\infty}^{\infty} \psi^{(i,\,j)} f(n_{\text{I}}, n_{\text{Q}})\, \mathrm{d}n_{\text{I}}\, \mathrm{d}n_{\text{Q}} \tag{26}$$

$$\psi^{(i,\,j)} = \begin{cases} 1, & \text{if } \varDelta = 0 \\ 0, & \text{else} \end{cases}, \qquad \varDelta = \min\left[d^{(i,\,k)},\ 0 \le k \le (M-1) \right] - d^{(i,\,j)} \tag{27}$$

where

$$f_{\mathrm{I}}(n_{\mathrm{I}}) = \frac{1}{\sqrt{2\pi}\,\sigma_{\mathrm{I}}}\exp\left[-\frac{n_{\mathrm{I}}^2}{2\sigma_{\mathrm{I}}^2}\right] \tag{28a}$$

$$f_{\mathrm{Q}}(n_{\mathrm{Q}}) = \frac{1}{\sqrt{2\pi}\,\sigma_{\mathrm{Q}}}\exp\left[-\frac{n_{\mathrm{Q}}^2}{2\sigma_{\mathrm{Q}}^2}\right] \tag{28b}$$

$$f(n_{\mathrm{I}}, n_{\mathrm{Q}}) = f_{\mathrm{I}}(n_{\mathrm{I}})f_{\mathrm{Q}}(n_{\mathrm{Q}}) \tag{28c}$$

$$\sigma_{\mathrm{I}} = \sigma_{\mathrm{Q}} = \frac{\sqrt{2}}{2}\sigma_{\mathrm{total}} \tag{28d}$$

where the superscripts of i, k and j denotes the i-th, k-th and j-th symbol points in the standard signal constellation, respectively. The variable of $d^{(i,k)}$ refers to the Euclidean distance between the actually received signal point and the signal constellation point of the j-th symbol when the i-th symbol is transmitted. The function $\min(d^{(i,k)}, 0 \le k \le (M-1))$ denotes the minimum value of $d^{(i,k)}$ for different values of k when $0 \le k \le (M-1)$. The random variables of n_{I} and n_{Q} refers to the in-phase and quadrature-phase (I-Q) components of total noise. σ_{total} is the standard deviation of the total noise. σ_{I} and σ_{Q} denotes to the in-phase and quadrature-phase (I-Q) components of σ_{total}. The functions of $f_{\mathrm{I}}(n_{\mathrm{I}})$ and $f_{\mathrm{Q}}(n_{\mathrm{Q}})$ are Gaussian probability density functions with respect to in-phase and quadrature-phase (I-Q) components of the total noise. The function of $P_{\mathrm{ro}}^{(i,j)}$ is the output probability of the j-th symbol constellation point when the i-th symbol point is transmitted.

$$\mathrm{BER} = \sum_{i=0}^{M-1}\sum_{j=0}^{M-1} B_{\mathrm{diff}}^{(i,j)}\, P_{\mathrm{ro}}^{(i)}\, P_{\mathrm{ro}}^{(i,j)} \tag{29a}$$

$$B_{\mathrm{diff}}^{(i,j)} = 1 - \frac{N_{\mathrm{same}}^{(i,j)}}{L_{\mathrm{enSym}}^{(i)}} \tag{29b}$$

where the variable of $P_{\mathrm{ro}}^{(i)}$ is the occurrence probability of the i-th symbol point. $N_{\mathrm{same}}^{(i,j)}$ is the number of the same bits when the input bit sequence corresponding to the i-th symbol point is compared bit-by-bit from left to right bits with that corresponding to the j-th symbol point. $L_{\mathrm{enSym}}^{(i)}$ is the number of input bits corresponding to the i-th symbol point. $B_{\mathrm{diff}}^{(i,j)}$ is called as the local error bit rate for the input bit sequence when the ith symbol point is wrongly decided to be the j-th symbol point. As examples, for 16QAM Huffman coding listed in Table 1, the values of $B_{\mathrm{diff}}^{(0,3)}$, $B_{\mathrm{diff}}^{(2,8)}$, $B_{\mathrm{diff}}^{(15,8)}$ and $B_{\mathrm{diff}}^{(7,15)}$ are respectively calculated to be 2/3, 1/3, 3/5 and 1/4. For simplicity, the total noises only include two kinds of noises in this paper. One is the FWM noise, and the other is the amplified spontaneous emission (ASE) noise coming from the cascaded erbium-doped fiber amplifiers (EDFAs). The power of the ASE noise can be expressed as

$$P_{\mathrm{ASE}} = S_{\mathrm{ASE}} B \tag{30a}$$

$$S_{\mathrm{ASE}} = N_{\mathrm{span}} h \nu n_{\mathrm{sp}} \Big[\exp(\alpha L) - 1\Big] \exp(-\alpha L) \tag{30b}$$

where S_{ASE} is the power spectral density (PSD) of ASE, B is bandwidth of optical filter, n_{sp} is spontaneous emission factor, h is Planck's constant, and v is optical frequency.

$$\sigma_{\mathrm{total}} \approx \sqrt{P_{\mathrm{FWM}} + P_{\mathrm{ASE}}} \tag{31}$$

The equivalent Q-factor is used to evaluate system performance in this paper, which can be expressed as

$$Q = \sqrt{2}\, \mathrm{erfcinv}(2 \times \mathrm{BER}) \tag{32}$$

where the function of erfcinv is the inverse complementary error function. Further, Q_{w} and Q_{wo} correspond to the values of Q that the impact of FWM noise is taken into account and not, respectively. In order to quantify the performance degradation due to FWM noise, a parameter of F_{QP} is given as

$$F_{\mathrm{QP}} = -10 \times \log_{10}(Q_{\mathrm{w}} / Q_{\mathrm{wo}}) \tag{33}$$

The spectral efficiency (SE) is expressed as

$$\mathrm{SE} = -\sum_{i=1}^{M} \Big[P_{\mathrm{ro}}^{(i)} \log_2(P_{\mathrm{ro}}^{(i)}) \Big] \tag{34}$$

The optimal value of P_{ave} corresponding to the maximum value of Q_{w} is written as $P_{\mathrm{ave}}^{\mathrm{opt}}$. The values of Q_{w} and F_{QP} corresponding to $P_{\mathrm{ave}}^{\mathrm{opt}}$ are written as $Q_{\mathrm{w}}^{\mathrm{max}}$ and $F_{\mathrm{QP}}^{\mathrm{opt}}$, respectively. In order to evaluate the performance gain in terms of $Q_{\mathrm{w}}^{\mathrm{max}}$ for case E over case F, a quantity of $R_{\mathrm{Q,\,E,\,F}}^{\mathrm{imp}}$ is defined as

$$R_{\mathrm{Q,\,E,\,F}}^{\mathrm{imp}} = 10 \log_{10}\left(\frac{Q_{\mathrm{w,\,E}}^{\mathrm{max}}}{Q_{\mathrm{w,\,F}}^{\mathrm{max}}} \right) \tag{35}$$

where $Q_{\mathrm{w,\,E}}^{\mathrm{max}}$ and $Q_{\mathrm{w,\,F}}^{\mathrm{max}}$ are the values of $Q_{\mathrm{w}}^{\mathrm{max}}$ corresponding to the case E and case F, respectively.

6. Numerical results and discussions

In the following, some example calculations for the proposed constellation shaped 16-ary signal in OFDM system with polarization-domain PCTW scheme are carried out by using the semi-analytic calculation models of FWM noise, BER and the equiv-

Table 3. Some system parameters and conditions.

Parameter	Value or status	Parameter	Value or status
Symbol rate	10 Gsym/s	OFDM subcarriers	128
Nonlinear coefficient	1.22 $W^{-1}km^{-1}$	Dispersion	16 ps/nm/km
Attenuation	0.2 dB/km	Length per span	100 km
n_{sp}	3	Transmission distance	5000 km
Polarization	Dual-polarization	Cyclic prefix of OFDM	Zero
Probabilistic shaping	Huffman coding	Geometric shaping	Included
Dispersion compensation	Digital	Nonlinear phase noises	Ignored

Table 4. Four cases of constellation shaping schemes.

	With radius-optimized geometric shaping	Without any geometric shaping
Without Hulfman coding	Case A (with Geo, without Hul)	Case B (without Geo, without Hul)
With Hulfman coding	Case C (with Geo, with Hul)	Case D (without Geo, with Hul)

alent Q-factor derived in this paper. Some system parameters and conditions in our calculations are given in Table 3. After each span, a EDFA is used to fully compensate for the loss of optical fibers within the whole span. Four cases of constellation shaping schemes listed in Table 4 are discussed in this paper. In order to realize the proposed

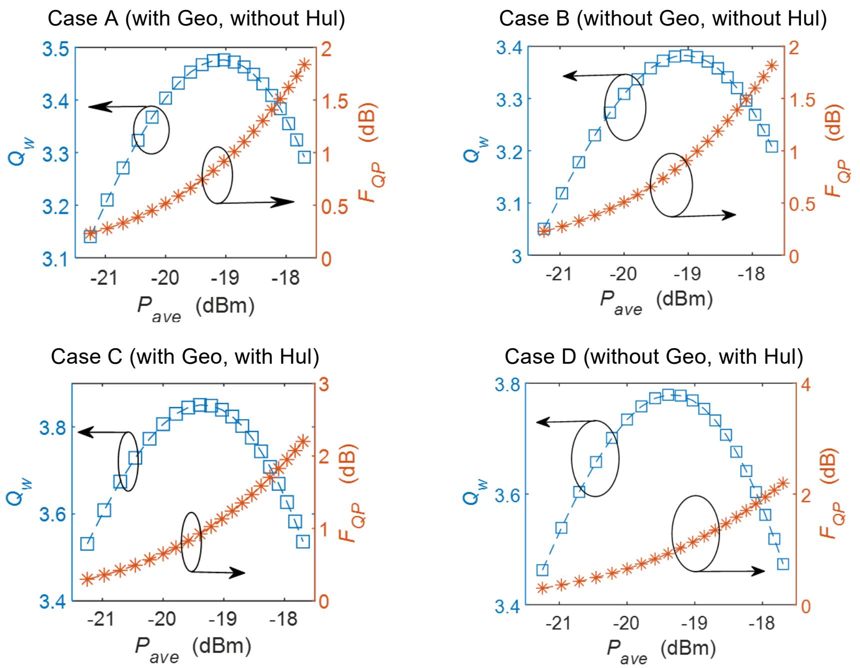

Fig. 2. Q_w and F_{QP} *versus* P_{ave} for 16-ary signal in PCTW OFDM system with four self-defined cases listed in Table 4.

radius-optimized geometric shaping scheme, the values of ε_1, ε_2 and ε_3 should be optimized. When the probabilistic shaping of Huffman coding is simultaneously adopted, the optimal values of ε_1, ε_2 and ε_3 are calculated to be –0.0481, –0.0440 and –0.0763, respectively, whereas for the case without any probabilistic shaping, the optimized values of ε_1, ε_2 and ε_3 are calculated to be –0.056, –0.124 and –0.070, respectively.

Values of Q_w and F_QP *versus* P_ave are derived and shown by Fig. 2. The values of $P_\mathrm{ave}^\mathrm{opt}$, $Q_\mathrm{w}^\mathrm{max}$, $F_\mathrm{QP}^\mathrm{opt}$ and SE are given by Table 5 for 16-ary PCTW OFDM system. The system performance gain can be obtained from Table 5. For example, the value of $Q_\mathrm{w}^\mathrm{max}$ is 3.383 for case B (without Geo, without Hul), whereas it is 3.851 for case C (with Geo, with Hul), so the value of the performance gain for case C (with Geo, with Hul) over case B (without Geo, without Hul), written as $R_\mathrm{Q,\,C,\,B}^\mathrm{imp}$, is 0.563 dB. Similarly, the performance gains of $R_\mathrm{Q,\,C,\,D}^\mathrm{imp}$, $R_\mathrm{Q,\,C,\,A}^\mathrm{imp}$, $R_\mathrm{Q,\,D,\,B}^\mathrm{imp}$, $R_\mathrm{Q,\,D,\,A}^\mathrm{imp}$ and $R_\mathrm{Q,\,A,\,B}^\mathrm{imp}$ are calculated to be 0.082, 0.445, 0.481, 0.363 and 0.118 dB, respectively. From the numerical results obtained above, it can be inferred that Huffman coding can be used to greatly improve system performance of 16-ary PCTW OFDM system at the expense of reduced SE whether or not the geometric shaping is used. The improvement of system performance by using the radius optimized geometric shaping is relatively limited, but the SE remains unchanged for it. When the Huffman-coded probabilistic shaping and radius-optimized geometric shaping are adopted simultaneously, the performance gain of 16-ary PCTW OFDM system is about 0.563 dB. Figure 3 shows that the deg-

T a b l e 5. Numerical results for 16-ary signal in PCTW OFDM system with four cases listed in Table 4.

	$P_\mathrm{ave}^\mathrm{opt}$ [dBm]	$Q_\mathrm{w}^\mathrm{max}$	$F_\mathrm{QP}^\mathrm{opt}$ [dB]	SE [bit/symbol]
Case A (with Geo, without Hul)	–19.031	3.476	0.961	4
Case B (without Geo, without Hul)	–19.031	3.383	0.905	4
Case C (with Geo, with Hul)	–19.393	3.851	0.925	3.75
Case D (without Geo, with Hul)	–19.393	3.779	0.922	3.75

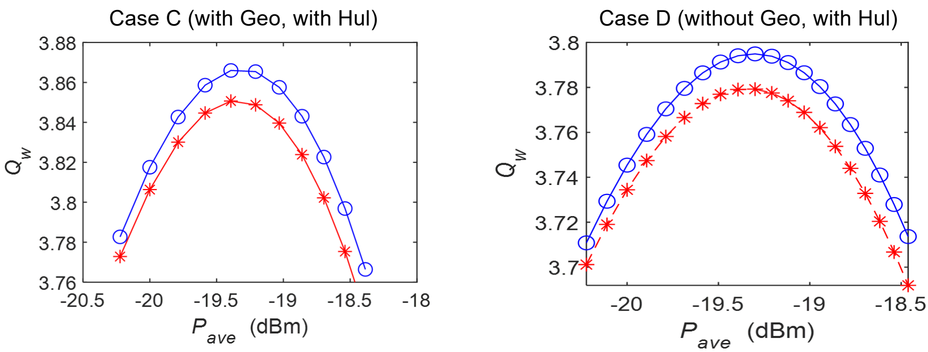

Fig. 3. Q_w *versus* P_ave for 16-ary signal in PCTW OFDM system with case C (with Geo, with Hul) and case D (without Geo, with Hul) where the marks of ∗ and ○ correspond to the cases of FWM models including and not including ISI, respectively.

radation of system performance due to the impact of ISI on FWM noise is relatively large when the values of P_{ave} are optimized.

7. Conclusion

Semi-analytic models are developed to calculate the variances of FWM noises for any probabilistic and geometric shaping centrosymmetric signal in PCTW OFDM system including walk-off and intersymbol interference. For any constellation shaped signal, the semi-analytic calculation models of BER and the equivalent Q-factor are derived also when the total noise is modeled as additive white Gaussian noise. The system performances of 16-ary OFDM system with polarization-domain PCTW scheme for different cases are evaluated when the impacts of the FWM and ASE noises are taken into accounted by using the newly derived calculation models. Our semi-analytic models can be further developed for constellation shaped signal in PCTW OFDM system when other techniques such as trellis coded modulation (TCM) and maximum posterior probability (MAP) algorithm are adopted simultaneously. The relevant calculations and discussions will be carried out in the future.

Acknowledgements
The authors gratefully acknowledge the financial supports in part: Natural Science Foundation of the Higher Education Institutions of Jiangsu Province, China (16kJB510033).

References

[1] SHIEH W., ATHAUDAGE C., *Coherent optical orthogonal frequency division multiplexing*, Electronics Letters **42**(10), 2006: 587-588. https://doi.org/10.1049/el:20060561
[2] PECHENKIN V., FAIR I.J., *On four-wave mixing suppression in dispersion-managed fiber-optic OFDM systems with an optical phase conjugation module*, Journal of Lightwave Technology **29**(11), 2011: 1678-1691. https://doi.org/10.1109/JLT.2011.2138677
[3] BOSCO G., CANO I.N., POGGIOLINI P., LI L., CHEN M., *MLSE-based DQPSK transmission in 43 Gb/s DWDM long-haul dispersion-managed optical systems*, Journal of Lightwave Technology **28**(10), 2010: 1573-1581. https://doi.org/10.1109/JLT.2010.2046475
[4] SONG H., BRANDT-PEARCE M., *Model-centric nonlinear equalizer for coherent long-haul fiber-optic communication systems*, [In] *2013 IEEE Global Communications Conference (GLOBECOM)*, Atlanta, GA, USA, 2013: 2394-2399. https://doi.org/10.1109/GLOCOM.2013.6831432
[5] IP E., *Nonlinear compensation using backpropagation for polarization-multiplexed transmission*, Journal of Lightwave Technology **28**(6), 2010: 939-951. https://doi.org/10.1109/JLT.2010.2040135
[6] LIU X., CHRAPLYVY A.R., WINZER P.J., TKACH R.W., CHANDRASEKHAR S., *Phase-conjugated twin waves for communication beyond the Kerr nonlinearity limit*, Nature Photonics **7**(7), 2013: 560-568. https://doi.org/10.1038/nphoton.2013.109
[7] LIU X., CHANDRASEKHAR S., WINZER P.J., TKACH R.W., CHRAPLYVY A.R., *Fiber-nonlinearity-tolerant superchannel transmission via nonlinear noise squeezing and generalized phase-conjugated twin waves*, Journal of Lightwave Technology **32**(4), 2014: 766-775. https://doi.org/10.1109/JLT.2013.2280998
[8] ELIASSON H., JOHANNISSON P., KARLSSON M., ANDREKSON P.A., *Mitigation of nonlinearities using conjugate data repetition*, Optics Express **23**(3), 2015: 2392-2402. https://doi.org/10.1364/OE.23.002392
[9] LIU X., *Twin-wave-based optical transmission with enhanced linear and nonlinear performances*, Journal of Lightwave Technology **33**(5), 2015: 1037-1043. https://doi.org/10.1109/JLT.2014.2383317

[10] TAVARES J.S., PESSOA L.M., SALGADO H.M., *Nonlinear compensation assessment in few-mode fibers via phase-conjugated twin waves*, Journal of Lightwave Technology **35**(18), 2017: 4072-4078. https://doi.org/10.1109/JLT.2017.2726758

[11] YOSHIDA T., SUGIHARA T., ISHIDA K., MIZUOCHI T., *Spectrally-efficient dual phase-conjugate twin waves with orthogonally multiplexed quadrature pulse-shaped signals*, [In] *OFC 2014*, San Francisco, CA, USA, 2014: 1-3. https://doi.org/10.1364/OFC.2014.M3C.6

[12] MATSUMINE T., YANKOV M.P., FORCHHAMMER S., *Geometric constellation shaping for concatenated two-level multi-level codes*, Journal of Lightwave Technology **40**(16), 2022: 5557-5566. https://doi.org/10.1109/JLT.2022.3179529

[13] SILLEKENS E., LIGA G., LAVERY D., BAYVEL P., KILLEY R.I., *High-cardinality geometrical constellation shaping for the nonlinear fibre channel*, Journal of Lightwave Technology **40**(19), 2022: 6374 -6387. https://doi.org/10.1109/JLT.2022.3197366

[14] FEHENBERGER T., ALVARADO A., BOCHERER G., HANIK N., *On probabilistic shaping of quadrature amplitude modulation for the nonlinear fiber channel*, Journal of Lightwave Technology **34**(21), 2016: 5063-5073. https://doi.org/10.1109/JLT.2016.2594271

[15] FU M., LIU Q., XU Y., JIANG H., ZENG X., WU Y., YI L., HU W., ZHUGE Q., *Multi-dimensional distribution matching with bit-level shaping for probabilistically shaped high order modulation formats*, Journal of Lightwave Technology **40**(9), 2022: 2870-2879. https://doi.org/10.1109/JLT.2022.3145621

[16] NAZARATHY M., KHURGIN J., WEIDENFELD R., MEIMAN Y., CHO P., NOE R., SHPANTZER I., KARAGODSKY V., *Phased-array cancellation of nonlinear FWM in coherent OFDM dispersive multi-span links*, Optics Express **16**(20), 2008: 15777-15810. https://doi.org/10.1364/OE.16.015777

[17] CHEN X., SHIEH W., *Closed-form expressions for nonlinear transmission performance of densely spaced coherent optical OFDM systems*, Optics Express **18**(18), 2010: 19039-19054. https://doi.org/10.1364/OE.18.019039

[18] LOWERY A.J., DU L.B.Y., *XPM efficiency versus symbol rate*, Journal of Lightwave Technology **40**(9), 2022: 2850-2861. https://doi.org/10.1109/JLT.2022.3148414

[19] SINKIN O.V., HOLZLOHNER R., ZWECK J., MENYUK C.R., *Optimization of the split-step Fourier method in modeling optical-fiber communications systems*, Journal of Lightwave Technology **21**(1), 2003: 61-68. https://doi.org/10.1109/JLT.2003.808628

[20] KUMAR S., *Analysis of degenerate four-wave-mixing noise in return-to-zero optical transmission systems including walk-off*, Journal of Lightwave Technology **23**(1), 2005: 310-320. https://doi.org/10.1109/JLT.2004.835742

[21] DU J., *Bit-pattern-dependent non-degenerate four-wave-mixing crosstalk in dispersion managed DWDM systems including walk-off*, Optics Communications **282**(14), 2009: 2983-2989. https://doi.org/10.1016/j.optcom.2009.04.019

[22] DU J., *Four-wave mixing noise in dispersion managed DWDM system including effect of randomly varying birefringence strength and orientation along fiber*, Optical Fiber Technology **19**(2), 2013: 109–114. https://doi.org/10.1016/j.yofte.2012.11.008

[23] AKHTAR A., PAVEL L., KUMAR S., *Modeling interchannel FWM with walk-off in RZ-DPSK single span links*, Journal of Lightwave Technology **26**(14), 2008: 2142-2154. https://doi.org/10.1109/JLT.2008.920127

[24] DU J., TENG Z., SHEN N., *Semi-analytic modeling of FWM noise in dispersion-managed DWDM systems with DQPSK/DPSK/OOK channels*, Optics Communications **358**, 2016: 180-189. https://doi.org/10.1016/j.optcom.2015.07.052

[25] DU J., SHEN N., XU Y., *Modeling interchannel four-wave mixing for 8-Ary modulated dense wavelength division multiplexing systems over dispersion map*, Optical Engineering **55**, 2016: 086111. https://doi.org/10.1117/1.OE.55.8.086111

[26] DU J., WANG Z., WU J., *Semi-analytic modeling of FWM noise in QAM Nyquist-WDM system with phase-conjugated twin waves*, Optics Communications **428**, 2018: 169-175. https://doi.org/10.1016/j.optcom.2018.07.049

[27] DU J., WU J., MIAO T., *Modeling inter-subcarrier four-wave mixing noises in QAM coherent OFDM system using phase-conjugated twin waves with diversity implement domains*, Optics Communications **450**, 2019: 261-268. https://doi.org/10.1016/j.optcom.2019.05.066

[28] POGGIOLINI P., BOSCO G., CARENA A., CURRI V., JIANG Y., FORGHIERI F., *The GN-model of fiber non-linear propagation and its applications*, Journal of Lightwave Technology **32**(4), 2014: 694-721. https://doi.org/10.1109/JLT.2013.2295208

Received August 27, 2023
in revised form October 22, 2023